# BLIND DECONVOLUTION OF FUNDAMENTAL AND HARMONIC ULTRASOUND IMAGES

*Mohamad Hourani*[1,2], *Adrian Basarab*[2], *Oleg Michailovich* [3], *Giulia Matrone*[4], *Alessandro Ramalli*[5] *Denis Kouamé* [2], *Jean-Yves Tourneret*[1]

[1] University of Toulouse, IRIT/INP-ENSEEIHT, 31071 Toulouse Cedex 7, France

[2] University of Toulouse, IRIT, CNRS UMR 5505, Université Paul Sabatier, Toulouse, France

[3] Department of Electrical and Computer Engineering, University of Waterloo, Canada

[4] Department of Electrical, Computer and Biomedical Engineering, University of Pavia, Italy

[5] Department of Cardiovascular Imaging and Dynamics, KU Leuven, Belgium

## ABSTRACT

Restoring the tissue reflectivity function (TRF) from ultrasound (US) images is an extensively explored research field. It is well-known that human tissues and contrast agents have a non-linear behavior when interacting with US waves. In this work, we investigate this non-linearity and the interest of including harmonic US images in the TRF restoration process. Therefore, we introduce a new US image restoration method taking advantage of the fundamental and harmonic components of the observed radiofrequency (RF) image. The depth information contained in the fundamental component and the good resolution of the harmonic image are combined to create an image with better properties than the fundamental and harmonic images considered separately. Under the hypothesis of weak scattering, the RF image is modeled as the 2D convolution between the TRF and the system point spread function (PSF). An inverse problem is formulated based on this model able to jointly estimate the TRF and the PSF. The interest of the proposed blind deconvolution algorithm is shown through an *in vivo* result and compared to a conventional US restoration method.

***Index Terms***— ultrasound imaging, harmonic ultrasound imaging, blind deconvolution, image restoration.

## 1. INTRODUCTION

Ultrasound (US) imaging is one of the main medical imaging modalities due to its abilities to non-invasively reveal anatomy and inspect the movement of organs and blood flow in real time with non-ionizing radiations, low cost, ease of use, and high frame rates. To obtain a US image, an electrical pulse, with central frequency $f_0$, is sent to the piezoelectric elements forming the US probe, pushing them to vibrate and thus to emit US waves. In US imaging, the interaction between the incident waves and the medium is nonlinear. The nonlinear behavior of the medium creates a distortion of the propagating waves. As a consequence of this distortion, new harmonic frequencies appear in the spectrum of received echoes. In practice, the study of these harmonics generally stops at the first harmonic $(2f_0)$ mainly because of the limited bandwidth of the transducers and of frequency dependent attenuation which is higher for higher harmonics. While contrast agents are used in clinics to increase tissue nonlinearity, several works showed that some tissues can cause sufficient distortion by themselves to generate harmonics, resulting into the so called tissue harmonic imaging (THI). Several methods have been already proposed to separate fundamental (around $f_0$) and harmonic (around $2f_0$) images. These methods include pulse inversion or phase cancellation, or post processing approaches like system identification or linear filtering in the case of low overlap between the spectra of the two images. Compared to fundamental US images, harmonic images have better spatial resolution and contrast, but suffer from higher attenuation and lower signal to noise ratio.

Specifically, the spatial resolution, contrast and signal to noise ratio of US images are affected by the limited bandwidth of the imaging transducer. In addition, US images are characterized by the so-called speckle, a granular pattern, which impacts on the image quality in terms of contrast and resolution. To overcome these limitations, a very rich literature exists, including post processing techniques based on image deconvolution. Such approaches consider, under the first order Born approximation, that beamformed radiofrequency (RF) images can be modelled as the 2D convolution between the tissue reflectivity function (TRF) and the point spread function (PSF). In practice, the PSF is unknown and can be pre-estimated from the data using methods such as minimum phase [1] or homomorphic filtering [2]. The latter works in the cepstrum domain, where the PSF presents a smooth behavior in contrast to the TRF that can be considered as noise. Parametric approaches have also been proposed to estimate the PSF, such as the parametric hybrid inverse filtering proposed in [3] or the Bayesian method in [4].

This work mainly proposes two contributions: 1) to take advantage of both fundamental and harmonic images in the TRF restoration process and 2) to propose a blind algorithm to jointly estimate the TRF and the phase of the PSF.

## 2. PROBLEM STATEMENT

### 2.1. US image formation model

Different models have been proposed in the literature to link RF images to TRF, by modelling the US propagation in the tissues [5]. These models use the first Born approximation that ignores multiple scattering [6] ans consider a spatially varying PSF [7]. The latter is generally further simplified in US image restoration algorithms to a 2D convolution between the TRF and a spatially invariant PSF, by restricting the deconvolution to image segments. Note that these convolution models are used in many US simulators [8, 9]. Interestingly, this convolution model was shown to also accurately describe the nonlinear propagation of US images in the context of low non linearity, which is the case of THI [10]. Based on these existing studies, the image formation models used in this work for fundamental and

harmonic images are defined as

$$\boldsymbol{y}_f = \boldsymbol{H}_f\boldsymbol{r} + \boldsymbol{n}_f \quad (1)$$

$$\boldsymbol{y}_h = \boldsymbol{W}\boldsymbol{H}_h\boldsymbol{r} + \boldsymbol{n}_h \quad (2)$$

where $\boldsymbol{y}_f$ and $\boldsymbol{y}_h \in \mathbb{R}^N$ are the observed fundamental and harmonic RF images, $\boldsymbol{r} \in \mathbb{R}^N$ is the TRF to be estimated and $\boldsymbol{n}_f$ and $\boldsymbol{n}_h \in \mathbb{R}^N$ are additive white Gaussian noises. $\boldsymbol{H}_f$ and $\boldsymbol{H}_h \in \mathbb{R}^{N\times N}$ are block circulant with circulant blocks matrices accounting for the fundamental and harmonic system PSFs, denoted in the following by $\boldsymbol{h}_f$ and $\boldsymbol{h}_h$ and $N$ is the number of samples. Due to the high attenuation of the harmonic image with depth, we consider in the second model a diagonal matrix $\boldsymbol{W} \in \mathbb{R}^{N\times N}$ whose diagonal elements account for the level of attenuation at each depth.

### 2.2. Problem reformulation

The objective of this paper is to solve a blind restoration problem to estimate jointly the PSFs $\boldsymbol{h_f}$ and $\boldsymbol{h_h}$ and the TRF $r$ from the observed RF images $\boldsymbol{y_f}$ and $\boldsymbol{y_h}$. Specifically, we express the joint blind deconvolution problem as the minimization of the following function

$$\min_{\boldsymbol{r},\boldsymbol{h_f},\boldsymbol{h_h}} \frac{1}{2}\|\boldsymbol{y_f} - \boldsymbol{H_f}\boldsymbol{r}\|_2^2 + \frac{1}{2}\|\boldsymbol{y_h} - \boldsymbol{W}\boldsymbol{H_h}\boldsymbol{r}\|_2^2 + \mu g(\boldsymbol{r}) \quad (3)$$

where the first two terms represent the fundamental and harmonics image data fidelity terms, $g(\boldsymbol{r})$ is a regularization term and $\mu$ a hyper-parameter controlling the weight of this regularization with respect to the two data fidelity terms. In this work, we consider a Laplacian prior distribution for the TRF, leading to an $\ell_1$-norm regularization in the function to minimize as in [11, 12].

## 3. OPTIMIZATION ALGORITHM

To solve the non convex optimization problem in (3), we propose in this work an alternating minimization method that estimates sequentially the PSFs and the TRF. To ensure the convergence towards a reliable solution, we use two constraints on the PSFs. Specifically, the magnitude of the Fourier transform of $\boldsymbol{h_f}$ and $\boldsymbol{h_h}$ are supposed known. These magnitudes can be pre-estimated from the fundamental and harmonic RF images by homomorphic filtering [2, 13]. Taking into account these two constraints, the problem in (3) can be written as

$$\begin{aligned} \min_{\boldsymbol{r},\boldsymbol{h}_f,\boldsymbol{h}_h} \quad & \tfrac{1}{2}\|\boldsymbol{y}_f - \boldsymbol{H}_f\boldsymbol{r}\|_2^2 + \tfrac{1}{2}\|\boldsymbol{y}_h - \boldsymbol{W}\boldsymbol{H}_h\boldsymbol{r}\|_2^2 + \mu\|\boldsymbol{r}\|_1 \\ s.t. \quad & |\mathcal{F}(\boldsymbol{h}_f)| = \widehat{\boldsymbol{h}}_f, \quad |\mathcal{F}(\boldsymbol{h}_h)| = \widehat{\boldsymbol{h}}_h \end{aligned} \quad (4)$$

where $\mathcal{F}(.)$ is the 2D Fourier transform operator and $\widehat{\boldsymbol{h}}_f$ and $\widehat{\boldsymbol{h}}_h$ are the Fourier transform magnitudes of the PSFs, which are estimated by applying homomorphic filtering to $\boldsymbol{y}_f$ and $\boldsymbol{y}_h$. The proposed optimization algorithm alternates between three steps that are summarized below

$$\boldsymbol{r}^* \in \min_{\boldsymbol{r}} \quad \tfrac{1}{2}\|\boldsymbol{y}_f - \boldsymbol{H}_f^*\boldsymbol{r}\|_2^2 + \tfrac{1}{2}\|\boldsymbol{y}_h - \boldsymbol{W}\boldsymbol{H}_h^*\boldsymbol{r}\|_2^2 + \mu\|\boldsymbol{r}\|_1 \quad (5)$$

$$\boldsymbol{h}_f^* \in \min_{\boldsymbol{H}_f} \quad \tfrac{1}{2}\|\boldsymbol{y}_f - \boldsymbol{H}_f\boldsymbol{r}^*\|_2^2 \quad s.t. \quad |\mathcal{F}(\boldsymbol{h}_f)| = \widehat{\boldsymbol{h}}_f \quad (6)$$

$$\boldsymbol{h}_h^* \in \min_{\boldsymbol{H}_h} \quad \tfrac{1}{2}\|\boldsymbol{y}_h - \boldsymbol{W}\boldsymbol{H}_h\boldsymbol{r}^*\|_2^2 \quad s.t. \quad |\mathcal{F}(\boldsymbol{h}_h)| = \widehat{\boldsymbol{h}}_h. \quad (7)$$

### 3.1. TRF estimation

In order to minimize (5), we propose to use an alternating direction method of multipliers (ADMM) [14, 15]. ADMM has been extensively used in the area of convex programming and can be summarized as follows

$$\begin{aligned} \min_{\boldsymbol{u},\boldsymbol{v}} \quad & f_1(\boldsymbol{u}) + f_2(\boldsymbol{v}) \\ \text{s.t.} \quad & \boldsymbol{A}\boldsymbol{u} + \boldsymbol{B}\boldsymbol{v} = \boldsymbol{c} \end{aligned} \quad (8)$$

where $f_1$ and $f_2$ are closed convex functions and $\boldsymbol{A}, \boldsymbol{B}$, $\boldsymbol{u}, \boldsymbol{v}$ and $\boldsymbol{c}$ are matrices and vectors of correct sizes. In order to adapt our problem to the ADMM framework, we rewrite (5) as follows [16]

$$\min_{\boldsymbol{u},\boldsymbol{v}} \frac{1}{2}\|\boldsymbol{y}_f - \boldsymbol{H}_f\boldsymbol{u}\|_2^2 + \frac{1}{2}\|\boldsymbol{y}_h - \boldsymbol{W}\boldsymbol{z}\|_2^2 + \mu\|\boldsymbol{w}\|_1 \quad (9)$$

where $\boldsymbol{z} = \boldsymbol{H}_h\boldsymbol{r}, \boldsymbol{w} = \boldsymbol{u} = \boldsymbol{r}$ and $\boldsymbol{v} = \begin{bmatrix}\boldsymbol{w}\\ \boldsymbol{z}\end{bmatrix}$. The reformulated problem can fit the ADMM framework by choosing $f_1(\boldsymbol{u}) = \frac{1}{2}\|\boldsymbol{y}_f - \boldsymbol{H}_f\boldsymbol{u}\|_2^2$, $f_2(\boldsymbol{v}) = \frac{1}{2}\|\boldsymbol{y}_h - \boldsymbol{W}\boldsymbol{z}\|_2^2 + \mu\|\boldsymbol{w}\|_1$, $\boldsymbol{A} = \begin{bmatrix}I_N\\ \boldsymbol{H}_h\end{bmatrix}$, $\boldsymbol{B} = \begin{bmatrix}-I_N & 0\\ 0 & -I_N\end{bmatrix}$ and $\boldsymbol{c} = \boldsymbol{0}_N$. By attaching the Lagragian multiplier $\boldsymbol{\lambda} = (\boldsymbol{\lambda}_1^T, \boldsymbol{\lambda}_2^T)^T \in \mathbb{R}^{2N}$ to the linear constraint, the augmented Lagrangian (AL) can be expressed as

$$\mathcal{L}_A(\boldsymbol{u}, \boldsymbol{v}, \boldsymbol{\lambda}) = f_1(\boldsymbol{u}) + f_2(\boldsymbol{v}) + \frac{\beta}{2}\|A\boldsymbol{u} + B\boldsymbol{v}^{\boldsymbol{k}} + \frac{\boldsymbol{\lambda}^{\boldsymbol{k}}}{\beta}\|_2^2. \quad (10)$$

ADMM consists of iteratively minimizing the AL with respect to $\boldsymbol{u}$, $\boldsymbol{v}$ followed by the update of the Lagrangian multiplier $\boldsymbol{\lambda}$. Thus, the minimization of (10) can be performed using the following steps
Step 1: Update $\boldsymbol{u}$ using an analytical solution in the Fourier domain [17].

$$\boldsymbol{u}^{\boldsymbol{k+1}} \in \operatorname{argmin}_{\boldsymbol{u}} \frac{1}{2}\|\boldsymbol{y_f} - H_f\boldsymbol{u}\|_2^2 + \frac{\beta}{2}\|A\boldsymbol{u} + B\boldsymbol{v}^{\boldsymbol{k}} + \frac{\boldsymbol{\lambda}^{\boldsymbol{k}}}{\beta}\|_2^2 \quad (11)$$

Step 2.1: Update $\boldsymbol{w}$ using the soft thresholding operator associated with the $\ell_1$-norm [18]

$$\boldsymbol{w}^{\boldsymbol{k+1}} \in \operatorname{argmin}_{\boldsymbol{w}} \mu\|\boldsymbol{w}\|_1 + \frac{\beta}{2}\|\boldsymbol{u}^{\boldsymbol{k+1}} - \boldsymbol{w} + \frac{\boldsymbol{\lambda_1^k}}{\beta}\|_2^2 \quad (12)$$

Step 2.2: Update $\boldsymbol{z}$ using an analytical solution [17].

$$\boldsymbol{z}^{\boldsymbol{k+1}} \in \operatorname{argmin}_{\boldsymbol{w}} \frac{1}{2}\|\boldsymbol{y_h} - W\boldsymbol{z}\|_2^2 + \frac{\beta}{2}\|H_h\boldsymbol{u}^{\boldsymbol{k+1}} - \boldsymbol{z} + \frac{\boldsymbol{\lambda_2^k}}{\beta}\|_2^2 \quad (13)$$

Step 3: Update the Lagrangian multiplier $\boldsymbol{\lambda}$ as

$$\boldsymbol{\lambda}^{\boldsymbol{k+1}} = \boldsymbol{\lambda}^{\boldsymbol{k}} + \beta(\boldsymbol{A}\boldsymbol{u}^{\boldsymbol{k+1}} + \boldsymbol{B}\boldsymbol{v}^{\boldsymbol{k+1}}). \quad (14)$$

### 3.2. PSF estimation

The mimization problems in (6) and (7) aim at estimating the phases of the PSFs. To solve them, we use an algorithm that was recently proposed in [19], inspired from [20]. The convolution equations in (6) and (7) can be expressed as a spatial convolution between the zero padded PSFs $\boldsymbol{h}_x \in \mathbb{R}^{N_1,N_2}$ (for $x \in \{h, f\}$), with the TRF map $\boldsymbol{r} \in \mathbb{R}^{N_1,N_2}$ where $N = N_1 \times N_2$. Using Paserval theorem

(6) and (7) can be expressed as

$$\min_{\mathcal{H}_f} \quad \tfrac{1}{2}\|\mathcal{Y}_f - \mathcal{H}_f \,.\, \mathcal{R}\|_2^2 \qquad s.t. \quad |\mathcal{H}_f| = \widehat{\boldsymbol{h}}_f \tag{15}$$

$$\min_{\mathcal{H}_h} \quad \tfrac{1}{2}\|\mathcal{Y}_h - \mathcal{H}_h \,.\, \mathcal{R}\|_2^2 \qquad s.t. \quad |\mathcal{H}_h| = \widehat{\boldsymbol{h}}_h \tag{16}$$

where $(.)$ denotes element wise multiplication, $\mathcal{R} = \mathcal{F}(\boldsymbol{r}^*)$, $\mathcal{H}_x = \mathcal{F}(\boldsymbol{h}_x)$, $\mathcal{Y}_f = \mathcal{F}(\boldsymbol{y}_f)$ and $\mathcal{Y}_h = \mathcal{F}(\boldsymbol{W}^{-1}\boldsymbol{y}_h)$. Using $\mathcal{H}_x = \widehat{\boldsymbol{h}}_x \,.\, e^{j\angle\mathcal{H}_x} = \widehat{\boldsymbol{h}}_x \,.\, U_x$, the previous equations can be rewritten as follows

$$\min_{U_f} \quad \tfrac{1}{2}\|\mathcal{Y}_f - (\mathcal{R} \,.\, \widehat{\boldsymbol{h}}_f) \,.\, U_f\|_2^2 \tag{17}$$

$$\min_{U_h} \quad \tfrac{1}{2}\|\mathcal{Y}_h - (\mathcal{R} \,.\, \widehat{\boldsymbol{h}}_h) \,.\, U_h\|_2^2 \tag{18}$$

Note that the minimizations in (17) and (18) are conducted with respect to the phase vectors $U_f$ and $U_h$. This reformulation shows that the PSF estimation problems are reduced to estimating the optimal phase of all-pass filters $U_f$ and $U_h$. The reader may refer to [19] for details about the algorithm able to solve the two problems above.

## 4. RESTORATION RESULTS

### 4.1. *In vivo* data

The data used in this work was acquired with the research scanner ULA-OP 256 (Departement of Information Engineering, University of Florence, Italy) connected to the wide band 192-element linear array probe LA533 (Esaote S.p.A., Florence, Italy), with a 110 % bandwidth centered at 8 MHz and a 245 $\mu$m pitch [21]. In transmission (TX), the beam was focused at 33 mm depth and apodized with a Hanning window. The TX signal was a 10-cycle sine burst at 5 MHz with Hanning tapering and peak amplitude of 90 Vpp. 384 RF lines were classically beamformed, resulting into RF images of size $384 \times 4480$ pixels. The sampling frequency was set at 78.125 MHz. The acquisition was done *in vivo* by scanning the carotid artery and jugular vein of a young healthy volunteer.

### 4.2. Quantitative metrics and comparison approach

In order to assess quantitatively the results, this paper considers two metrics referred to as resolution gain (RG) and contrast-to-noise ratio (CNR). The RG is the ratio of the normalized autocorrelation (higher than 3 dB) of the original RF US image to the normalized autocorrelation (higher than 3 dB) of the restored TRF. An improvement in the resolution of the restored TRF corresponds to an RG higher than 1. To assess the improvement in contrast, we consider the CNR between two regions, e.g., the red and blue regions in Fig.1(e).

The results obtained using the proposed algorithm were compared to a conventional deconvolution algorithm using the fundamental RF image only. This classical method (referred to as LASSO) estimates the TRF by solving the following optimization problem

$$\min_{\boldsymbol{r},\boldsymbol{H}_f} \frac{1}{2}\|\boldsymbol{y}_f - \boldsymbol{H}_f\boldsymbol{r}\|_2^2 + \mu\|\boldsymbol{r}\|_1. \tag{19}$$

Note that the matrix $\boldsymbol{W}$ needed within the proposed restoration method, accounting for harmonic attenuation, was estimated from the original images before filtering by computing the ratio between the energy of the fundamental and the harmonic. These energies are estimated using the spectra of $\boldsymbol{y}_f$ and $\boldsymbol{y}_h$ within an axial moving block all along the image.

### 4.3. Results

The native fundamental and harmonic images, as well as the restored images, are displayed in Fig.1. Note that all the images are shown in B-mode. The corresponding quantitative metrics are shown in Table 1. The restoration of the fundamental image using LASSO presents a good resolution compared to the native fundamental image. However, the proposed solution presents an improvement in resolution compared to all the other images, including the one obtained by LASSO and the native harmonic image. In particular, the jugular vein and the carotid artery are better defined on the image restored with the proposed algorithm. Specifically, the proposed method shows a good resolution thanks to the harmonic image, and provides a non-attenuated restored image at high depth thanks to the fundamental image. The quantitative metrics in Table 1 highlight the improvement in CNR and in RG compared to fundamental and harmonic images, as well as to the LASSO solution.

Fig. 2 shows the estimated PSFs obtained with the proposed algorithm, by comparison to the pre-estimated PSFs with zero phase using homomorphic filtering. The proposed blind deconvolution approach is able to estimate the unknown phases of the PSFs, which is very promising. Note that the execution time of the proposed method is 130 seconds when using standard 3.6 GHz Intel Core i7 with a straightforward MATLAB implementation without GPU.

| | **LASSO** | **Proposed method** |
|---|---|---|
| **CNR** | 5.84 | **12.620** |
| **RG/Fundamental** | 2.448 | **3** |
| **RG/Harmonic** | 1.48 | **1.857** |

**Table 1**. Quantitative results corresponding to the selected regions (in red) of images in Figs. 1(c), (d).

## 5. CONCLUSION

This work showed the interest of combining harmonic and fundamental images for the blind restoration of the TRF in US imaging. Taking into account the attenuation in depth of harmonic images and the low resolution of fundamental images, the proposed method provides images with relatively low attenuation effect, better contrast, and with better spatial resolution than the native images. Future work will be devoted to explore a spatially variant deconvolution algorithm and to take into account two different TRFs for the fundamental and harmonic image models.

## 6. REFERENCES


[1] J. A. Jensen and S. Leeman, "Nonparametric estimation of ultrasound pulses," *IEEE Trans. Biomed. Eng.*, vol. 41, no. 10, pp. 929–936, 1994.

[2] T. Taxt, "Restoration of medical ultrasound images using two-dimensional homomorphic deconvolution," *IEEE Trans. Ultrason., Ferroelect., Freq. Control*, vol. 42, no. 4, pp. 543–554, 1995.

[3] O. Michailovich and A. Tannenbaum, "Blind deconvolution of medical ultrasound images: A parametric inverse filtering approach," *IEEE Trans. Image Process.*, vol. 16, no. 12, pp. 3005–3019, 2007.

[4] N. Zhao, Q. Wei, A. Basarab, D. Kouamé, and J.-Y. Tourneret, "Blind deconvolution of medical ultrasound images using a parametric model for the point spread function," in *Proc. IEEE Ultrason. Symp. (IUS), Tours, France*, Sept., 2016, pp. 1–4.

[5] B. E. Treeby, M. Tumen, and B. T. Cox, "Time domain simulation of harmonic ultrasound images and beam patterns in 3d using the k-space pseudospectral method," in *Int. Conf. Medical Image Computing and Computer-Assisted Intervention (MICCAI)*, Toronto, Canada, 2011.

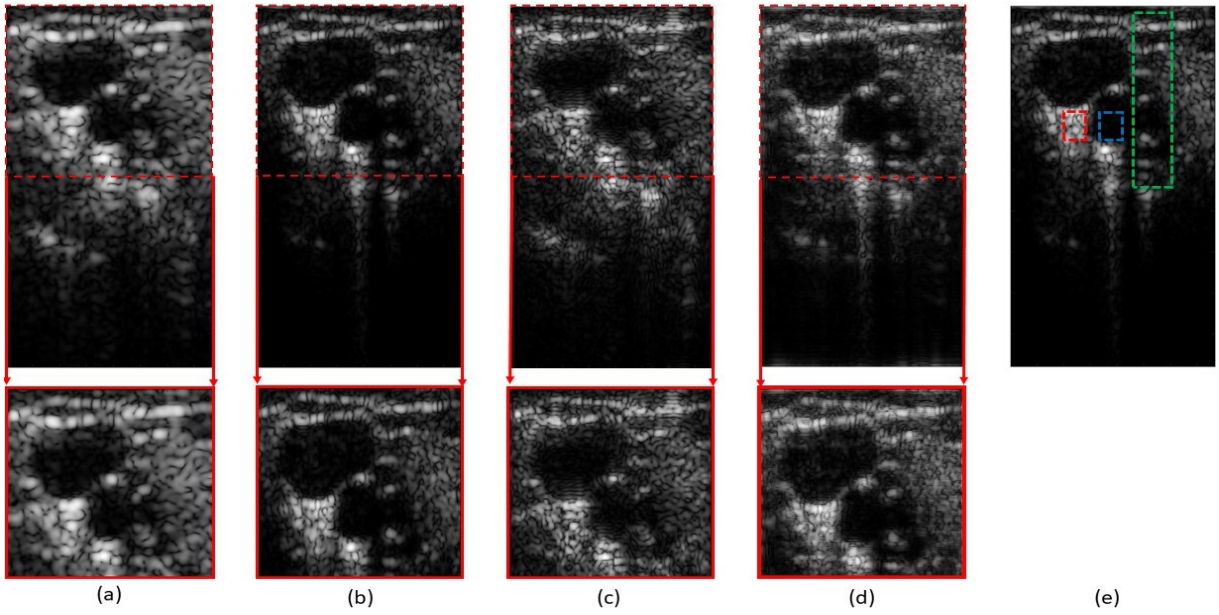


**Fig. 1**. (a) Fundamental image, (b) harmonic image, (c) blind LASSO restoration of the fundamental image, (d) blind restoration with the proposed method, (e) regions (red and blue blocks for CNR, green block for RG) used for quantitative metric computation ($\mu = 0.5, \beta = 0.1$).

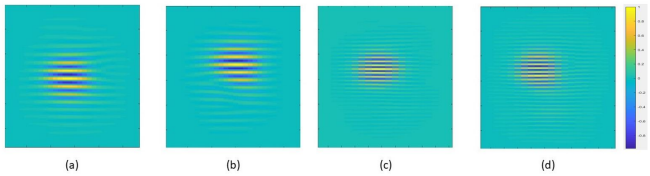


**Fig. 2**. (a) Zero phase fundamental PSF $\widehat{\boldsymbol{h}}_f$, (b) Estimated fundamental PSF $h_f$, (c) Zero phase harmonic PSF $\widehat{\boldsymbol{h}}_h$, (d) Estimated harmonic PSF $h_h$.


[6] P. R. Stepanishen, "The time-dependent force and radiation impedance on a piston in a rigid infinite planar baffle," *The Journal of the Acoustical Society of America*, vol. 49, no. 3B, pp. 841–849, 1971.

[7] J. A. Jensen and N. B. Svendsen, "Calculation of pressure fields from arbitrarily shaped, apodized, and excited ultrasound transducers," *IEEE Trans. Ultrason. Ferroelectr. Freq. Control*, vol. 39, no. 2, pp. 262–267, 1992.

[8] J. A. Jensen, "Field: A program for simulating ultrasound systems," in *Med. Biol. Eng. Comput.*, vol. 34, Supplement 1, Part 1: 351–353, 1996.

[9] F. Varray, A. Ramalli, C. Cachard, P. Tortoli, and O. Basset, "Fundamental and second-harmonic ultrasound field computation of inhomogeneous nonlinear medium with a generalized angular spectrum method," *IEEE Trans. Ultrason. Ferroelectr. Freq. Control*, vol. 58, no. 7, pp. 1366–1376, 2011.

[10] R. J. Zemp, C. K. Abbey, and M. F. Insana, "Linear system models for ultrasonic imaging: Application to signal statistics," *IEEE Trans. Ultrason. Ferroelectr. Freq. Control*, vol. 50, no. 6, pp. 642–654, 2003.

[11] R. Morin, S. Bidon, A. Basarab, and D. Kouamé, "Semi-blind deconvolution for resolution enhancement in ultrasound imaging," in *IEEE Proc. Int. Conf. Image Process. (ICIP)*, Melbourne, Australia, Feb. 2013.

[12] Z. Chen, A. Basarab, and D. Kouamé, "Compressive deconvolution in medical ultrasound imaging," *IEEE Trans. Med. Imag.*, vol. 35, no. 3, pp. 728–737, 2016.

[13] O. V. Michailovich and D. Adam, "A novel approach to the 2-D blind deconvolution problem in medical ultrasound," *IEEE Trans. Med. Imag.*, vol. 24, no. 1, pp. 86–104, 2005.

[14] D. Gabay and B. Mercier, "A dual algorithm for the solution of nonlinear variational problems via finite element approximation," *Computers & Mathematics with Applications*, vol. 2, no. 1, pp. 17–40, 1976.

[15] S. Boyd, N. Parikh, E. Chu, B. Peleato, and J. Eckstein, "Distributed optimization and statistical learning via the alternating direction method of multipliers," *Foundations and Trends in Machine Learning*, vol. 3, no. 1, pp. 1–122, 2011.

[16] M. Hourani, A. Basarab, D. Kouamé, J.-M. Girault, and J.-Y. Tourneret, "Restoration of ultrasonic images using non-linear system identification and deconvolution," in *Proc. Int. Symp. Biomedical Imaging (ISBI 2018), Washington D.C., USA*, April 4-7, 2018, pp. 1166–1169.

[17] M. Hourani, A. Basarab, D. Kouamé, and J.-Y. Tourneret, "Tissue reflectivity function restoration from fundamental and harmonic ultrasound images," in *The Signal Processing with Adaptive Sparse Structured Representations (SPARS) workshop, Toulouse, France*, July 4-7, 2019, https://www.irit.fr/ Adrian.Basarab/img/Spars2019_MH.pdf.

[18] Z. Chen, A. Basarab, and D. Kouamé, "Reconstruction of enhanced ultrasound images from compressed measurements using simultaneous direction method of multipliers," *IEEE Trans. Ultrason., Ferroelect., Freq. Control*, vol. 63, no. 10, pp. 1525–1534, Oct 2016.

[19] O. Michailovich, A. Basarab, and D. Kouame, "Iterative reconstruction of medical ultrasound images using spectrally constrained phase updates," in *Proc. IEEE Int. Symp. Biomed. Imaging (ISBI), Venice, Italy*, 8-11 Apr., 2019, pp. 1765–1768.

[20] S.-C. Pei and J.-J. Shyu, "Eigenfilter design of 1-D and 2-D IIR digital all-pass filters," *IEEE Trans. Signal Process.*, vol. 42, no. 4, pp. 966–968, 1994.

[21] G. Matrone, A. Ramalli, P. Tortoli, and G. Magenes, "Experimental evaluation of ultrasound higher-order harmonic imaging with filtered-delay multiply and sum (F-DMAS) non-linear beamforming," *Ultrasonics*, vol. 86, May 2018.